

**Linear Polarization of CMB and 21cm
&
Circular Polarization of CMB**

Soma De

*Post-doctoral Fellow, Arizona State University
presentation at 27th Texas Symposium, Dec 11, 2013*

Collaboration:

Levon Pogosian (*Dept of Physics, SFU*)

Hiroyuki Tashiro (*Dept of Physics, ASU*)

Tanmay Vachaspati (*Dept of Physics, ASU*)

ArXiv: (SD,LP,TV) <http://arxiv.org/abs/1305.7225>

ArXiv: (SD, HT) <http://arxiv.org/abs/1307.3584>

Basics of Faraday Rotation

- The direction of linear polarization vector is rotated as CMB passes through ionized medium permeated by magnetic field. Faraday rotation vs temperature anisotropy due to magnetic field :

CMB temperature anisotropy $\rightarrow B_{PMF} < \text{few nG}$ sourced by magnetic energy **quadratic** in field strength.

Faraday rotation is linear in field strength

- **Angle of rotation** along a line of sight is proportional to the line integral of **comoving magnetic field** ($\mathbf{B}(\mathbf{z}) = \mathbf{B}_{\text{obs}}(1+z)^2$) times **square** of the **observed wavelength**

- Symbolically

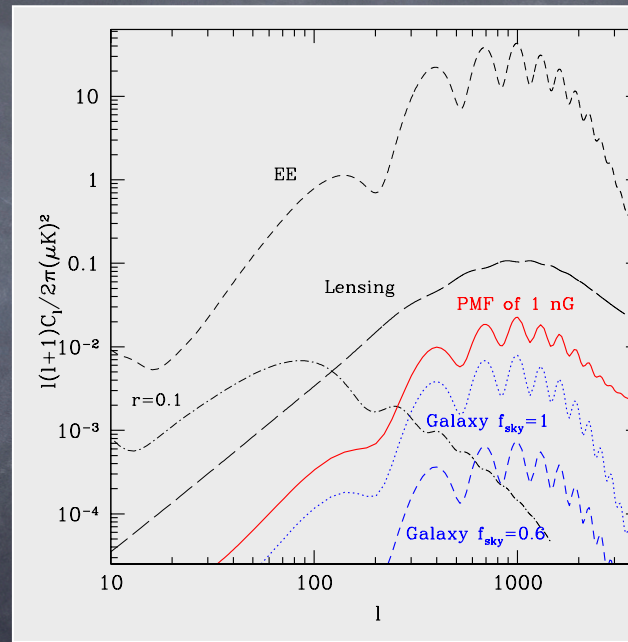
$$\alpha(\hat{\mathbf{n}}) = \lambda_0^2 RM(\hat{\mathbf{n}}) = \frac{3}{16\pi^2 e} \lambda_0^2 \int \hat{\tau} \cdot \mathbf{B} \cdot d\mathbf{l}$$

- τ is the optical depth, depends on the free electron density of the medium.

CMB B-mode spectra at 30GHz due to Faraday Rotation caused by primordial and Milky way magnetic field

Galactic RM data is from Oppermann et al (2012)

PMF (1 nG) B-mode peak power $\approx 0.03(\mu\text{K})^2$
Galactic (RM $\approx 30 \text{ rad/m}^2$) and at 30GHz gives a rotation angle $3 \times 10^{-3} \text{ rad}$.
B-mode peak power $\approx 0.01 (\mu\text{K})^2$
PMF is assumed to be scale-invariant.
Similar shape of B-mode spectra from PMF and Galactic magnetic field.



Galactic RM detection

Name - freq (GHz)	f_{sky}	FWHM (arcmin)	$\Delta_P (\mu\text{K-arcmin})$	$(S/N)_{EB} (+DL)$	$(S/N)_{TB} (+DL)$	$(S/N)_{BB} (+DL)$
Planck LFI - 30	0.6	33	240	5.3E-4 (same)	2.2E-3 (same)	2.3E-4 (same)
Planck HFI - 100	0.7	9.7	106	1.4E-3 (same)	7.5E-4 (same)	6E-5 (same)
Polarbear - 90	0.024 ^a	6.7	7.6	1.3E-2 (1.5E-2)	1.6E-3 (2.0E-3)	4.6E-4 (6.0E-4)
QUIET II - 40	0.04 ^a	23	1.7	0.3 (0.8)	0.05 (0.2)	0.02 (0.08)
CMBPOL - 30	0.6	26	19	1.0 (same)	0.4 (same)	0.05 (same)
CMBPOL - 45	0.7	17	8.25	2.1 (2.3)	0.8 (0.9)	0.12 (0.15)
CMBPOL - 70	0.7	11	4.23	2.0 (2.6)	0.6 (0.9)	0.08 (0.14)
CMBPOL - 100	0.7	8	3.22	1.4 (2.0)	0.3 (0.6)	0.03 (0.07)
Suborbital - 30	0.1	1.3	3	2.0 (3.1)	0.3 (0.7)	0.08 (0.2)
Space - 30	0.6	4	1.4	18 (28)	7 (14)	5 (30)
Space - 90	0.7	4	1.4	3.3 (6.8)	1.0 (2.4)	0.09 (0.64)

TABLE I: S/N of the overall detection of the galactic RM spectrum with Planck, Polarbear, QUIET, CMBPOL and optimistic future sub-orbital and space experiments. Results are presented without and with (+DL) de-lensing by a factor $f_{\text{DL}} = 0.01$. (^a based on 0.1 of RM sky.)

(+DL) $\rightarrow f_{\text{DL}} = 0.01$

2 σ bounds on effective PMF

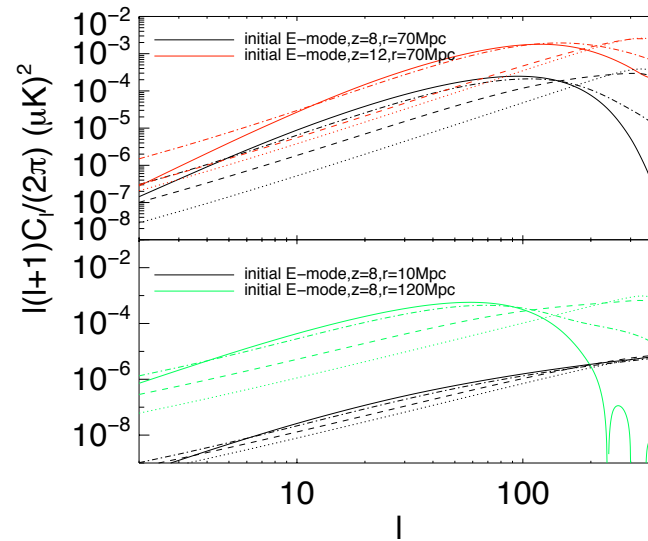
Name - freq (GHz)	$f_{\text{sky}} (f_{\text{sky}}^{\text{opt}})$	FWHM (arcmin)	$\Delta_P (\mu\text{K-arcmin})$	$B_{\text{eff}} (2\sigma, \text{nG})$	+DL (nG)	+DL+DG (nG)
Planck LFI - 30	0.6	33	240	16 ^b	same	same
Planck HFI - 100	0.7	9.7	106	23	same	same
Polarbear - 90	0.024 ^a	6.7	7.6	3.3	3.0	same
QUIET II - 40	0.04 ^a	23	1.7	0.46	0.26	0.25
CMBPOL - 30	0.6	26	19	0.56	0.55	0.51
CMBPOL - 45	0.7	17	8.25	0.38	0.35	0.29
CMBPOL - 70	0.7	11	4.23	0.39	0.32	0.26
CMBPOL - 100	0.7	8	3.22	0.52	0.4	0.34
Suborbital - 30	0.1	1.3	3	0.09	0.07	0.05
Suborbital - 90	0.1	1.3	3	0.63	0.45	same
Space - 30	0.6 (0.2)	4	1.4	0.06	0.04	0.02
Space - 90	0.7 (0.4)	4	1.4	0.26	0.15	0.12

$$f_{\text{DG}} = 0.1, f_{\text{DL}} = 0.01$$

ArXiv: (SD,LPTV) <http://arxiv.org/abs/1305.7225>

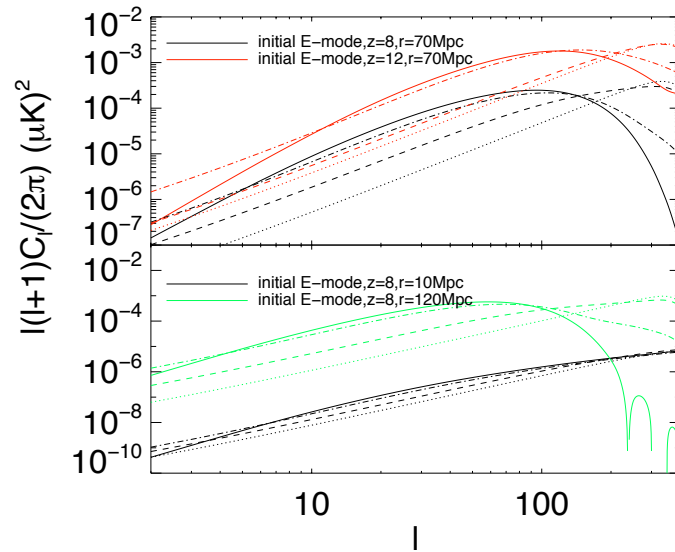
Recovery of MW RM from CMB polarization data: De and Mauskopf, Dec 2013, in prep

E-mode polarization spectra of 21 cm photons after they pass through the Milky Way



Solid lines indicate the initial E-modes. Dotted, dashed and dash-dotted lines indicate generated E-mode when RM is 100, 10, 1 percent of the actual value. The peak scale corresponds to the typical size of the ionized bubbles.

B-mode polarization spectra of 21 cm photons after they pass through the Milky Way



Solid lines indicate the initial E-modes. Dotted, dashed and dash-dotted lines indicate generated B-mode when RM is 100, 10, 1 percent of the actual value.

ArXiv: (SD, HT) <http://arxiv.org/abs/1307.3584>

Circular polarization of CMB ?

- ◆ Magnetic field, relativistic electrons due to the process of Faraday conversion creates circular polarization in CMB.
- ◆ We don't expect CMB to have circular polarization at the surface of last scattering. Current upper limit on $V/T_{\text{CMB}} \sim 10^{-4}$ (Ref: Mainini, 2013) using MIPOL at Testa Grigia observatory at the Italian Alps.
- ◆ The Milky way magnetic field is too small to generate any significant effect.
- ◆ Explosion of first stars have good prospects of generating conditions for CMB circular polarization. Therefore could CMB circular polarization be a good probe for the unobserved first stars? Could galaxy clusters be a significant source as well?

Steps to get to the V-parameter, the degree of circular polarization

Linear polarization of CMB

$$\frac{dV}{ds}(z, \vec{x}, \vec{n}) = U(z, \vec{x}, \vec{n}) \delta K_r(z, \vec{x}, \vec{n}, \vec{n}_B)$$

Path length to the observers

Properties of the first stars or the galaxies

$$\delta K_r \Rightarrow (N_r^{tot}, \gamma_L, B, \theta_B, \nu_L, \nu, \beta) \quad \text{(Sazonov, 1969)}$$

number density of the relativistic electrons

lower limit of the Lorentz factor

Angle between line of sight and B

frequency of the CMB photons

Larmor's frequency

spectral index of the relativistic electrons

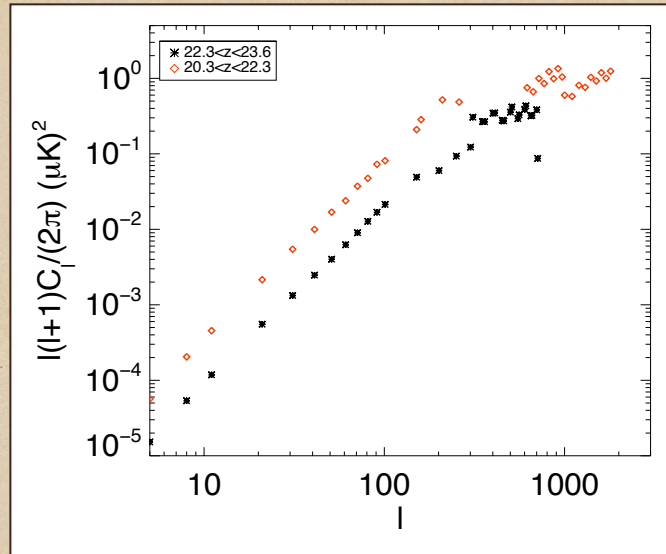
$$C_l^{VV} = \langle V_{lm} V_{lm}^* \rangle \Rightarrow (P(k), P_\alpha, P_{E_{lm}}) \quad \text{(De & Tashiro, in prep, Dec 2013)}$$

growth of structure

First star astrophysics

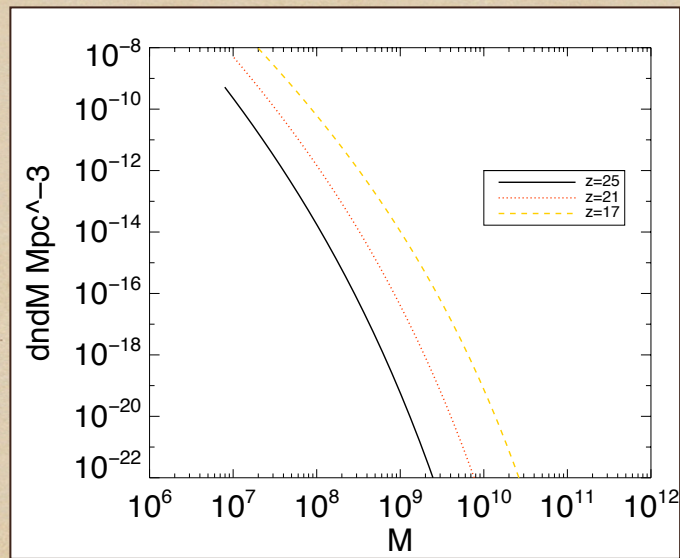
linear polarization

Predicted Signal of V

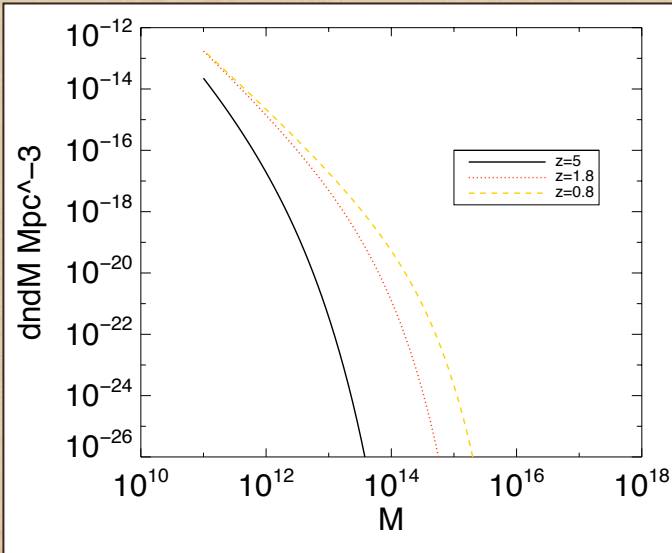


semi-analytic

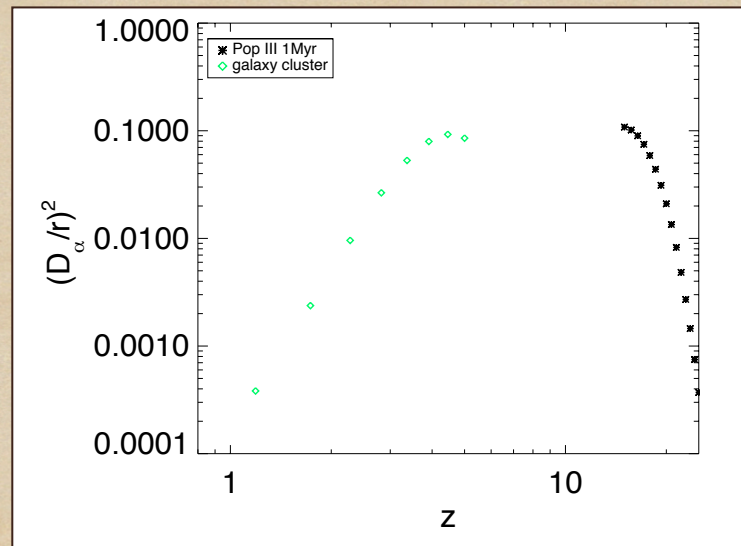
Number density per mass bin



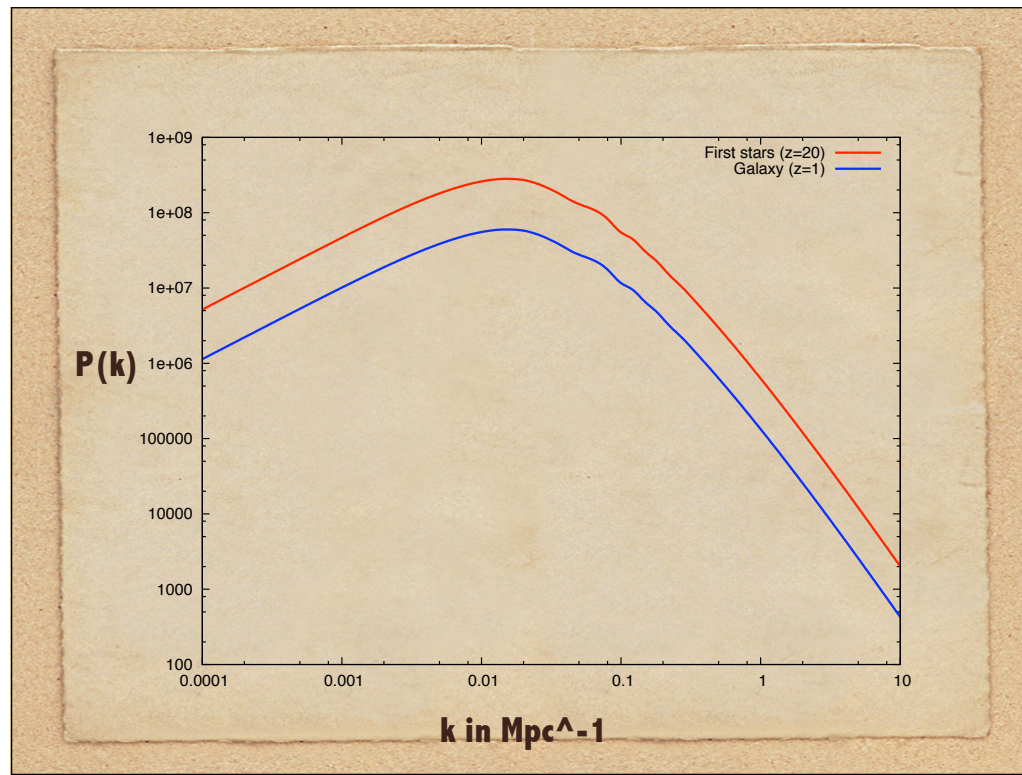
Number density per mass bin of galaxy clusters



Comparison of Astrophysical contributions



semi-analytic



Conclusion and Future prospects

- ◆ Low frequency measurement of V signal at high multipoles is a relatively foreground free way to detect the first stars and unique frequency signature (De and Tashiro in prep, 2013).

back up slides

Astrophysical Magnetic Fields

magnetic field in Gauss

10^{-9} 10^{-6} 10^{-3} 1 10^3 10^6 10^9

Voids Clusters, Galaxies stars white dwarfs Neutron stars

10^{26} 10^{25}
 10^{23} 10^{10} 10^9 10^6

linear size in cm

10^{13} 1 1 1
 10^{11}

mass in solar mass units

⊙ Magnetic fields are prevalent in galaxies and galaxy clusters. Field strengths are typically $1\mu\text{G}$ and $1-10\mu\text{G}$ with coherence lengths of 1 Kpc and $10-100$ Kpc respectively

How to recover faraday rotation angle from CMB data ?

Stokes parameters and Observations

Stokes parameters Q, U and V characterizing polarization

Explore the rotation of the linear polarization in different frequency channels (De and Mauskopf, 2013 in prep)

At a given frequency band explore the coupling between E-modes and Faraday rotation (FR) induced B-modes.

$$\alpha(\hat{n}) = \sum_{L,M} \alpha_{LM} Y_{LM}(\hat{n})$$

$$B_{lm} = 2 \sum_{LM} \sum_{l'm'} \alpha_{LM} E_{l'm'} \xi_{lm'l'm'}^{LM} H_{ll'}^L$$

$$\xi_{lm'l'm'}^{LM} \equiv (-1)^m \sqrt{\frac{(2l+1)(2L+1)(2l'+1)}{4\pi}} \times \begin{pmatrix} l & L & l' \\ -m & M & m' \end{pmatrix}$$

$$H_{ll'}^L \equiv \begin{pmatrix} l & L & l' \\ 2 & 0 & -2 \end{pmatrix}.$$

Therefore extract the rotation at a given point in sky by exploring coupling between E and B-modes from a given realization under small angle approximation

In the detection process of PMF Milky way magnetic field is an important foreground whose nature needs to be investigated.

B-mode spectra (PMF)

Stochasticity and isotropy allows us to write

$$\begin{aligned}\langle B_{l'm'}^* B_{lm} \rangle &= 4 \sum_{LM} \sum_{L'M'} \sum_{l_2 m_2} \sum_{l_2' m_2'} \xi_{lm l_2 m_2}^{LM} H_{ll_2}^L \xi_{l'm' l_2' m_2'}^{L'M'} H_{l'l_2'}^{L'} \langle \alpha_{LM}^* E_{l_2 m_2} \alpha_{L'M'} E_{l_2' m_2'} \rangle \\ &= \delta_{ll'} \delta_{mm'} 4 \sum_L \frac{(2L+1)}{4\pi} C_L^{\alpha\alpha} \sum_{l_2} (2l_2+1) C_{l_2}^{EE} (H_{ll_2}^L)^2\end{aligned}$$

$$C_l^{BB} = \frac{1}{\pi} \sum_L (2L+1) C_L^{\alpha\alpha} \sum_{l_2} (2l_2+1) C_{l_2}^{EE} (H_{ll_2}^L)^2$$

E,B-mode spectra (21 cm)

Fluctuations of neutral are only due to baryonic density and ionization fluctuations, hence only E-modes. Polarization due to ionization fluctuations dominate at EoR. This depends on EoR models.

$$C_l^{E,i}(\nu) = \frac{2}{\pi} \int k^2 dk [x_H^2 P_\delta(k) (\Delta_\delta^E(k, \nu))^2 + P_x(k) (\Delta_x^E(k, \nu))^2]$$

$$C_l^{BB,obs} = \sum_L \frac{2L+1}{4\pi} C_L^{\sin(2\alpha)} \sum_{l'} (2l'+1) C_{l'}^{EE} (H_{ll'}^L)^2$$

$$C_l^{EE,obs} = \sum_L \frac{2L+1}{4\pi} C_L^{\cos(2\alpha)} \sum_{l'} (2l'+1) C_{l'}^{EE} (H_{ll'}^L)^2$$